Harmonics analysis of 130-year hourly air temperature in Hong Kong: detecting urban warming from the perspective of annual and daily cycles

Article

Accepted Version

1 **Harmonics analysis of 130-year hourly air temperature in Hong Kong:**

2 **detecting urban warming from the perspective of annual and daily cycles**

3 **Kai Wang[1], Yuguo Li[1*], Zhiwei Luo[2], Shi Yin[1], Pak Wai Chan[3]**

4 1 Department of Mechanical Engineering, the University of Hong Kong, Pokfulam, Hong Kong,

5 China

6 2 School of the Built Environment, University of Reading, Reading, United Kingdom

7 3 Hong Kong Observatory, Hong Kong, China

8 * Corresponding author, E-mail: liyg@hku.hk. Tel: +852-39172625

9 **Abstract**

10   The century-long search for the precise mechanisms responsible for urban heat islands

11 continues, while urban warming worsens in many megacities. Most studies have focused on mean

12 temperature, daily and annual temperature ranges and urban heat island intensity. We hypothesize

13 that an analysis of the changes in the characteristics of the complete daily and annual temperature

14 cycles, including not only the mean temperature and temperature ranges (amplitudes) but also the

15 maximum and minimum temperatures and the phases, can provide more information on urban

16 warming phenomena. Through a detailed analysis of long-term observations in Hong Kong, we

17 found that the difference in the daily cycle between urban and rural stations is very distinct,

18 whereas the annual cycles are much more similar, suggesting that the urban environment has a

19 greater effect on the daily cycle than on the annual cycle. The daily phase has shifted a total of

20 1.77 hours later over the last 130 years (1.36 hours per century) in the urban area of Hong Kong

21 according to the Hong Kong Observatory (HKO) data. The annual phase change at HKO reflects

22 the globally observed phenomenon that the annual phase advances or seasons onset earlier.

23 **Keywords**

24 Urban warming   Daily temperature cycle   Annual temperature cycle   Phase lag

1 Introduction

Ongoing urban warming has been well documented in many studies. Urban areas are widely recognized as being much warmer than their surrounding rural areas, which is known as the urban heat island (Oke 1987). The diurnal temperature range (DTR) is smaller in urban than in rural areas due to the higher daily minimum temperature (Gallo et al. 1996). In decadal time scales, urban areas experience a greater increasing trend in daily mean temperature and a larger decreasing trend in DTR compared with rural areas or the global average (Easterling et al. 1997; Jones et al. 1990; Wang et al. 2012). Therefore, the larger magnitude changes in the mean temperature and DTR are considered to be the major indicators of urban climate change and have thus been intensively studied.

Understanding the mechanisms that cause the various phenomena involved in urban warming is critical to identifying the anthropogenic effect and natural variation in climate change. Urban areas have larger areas of impervious land, higher emission of greenhouse gases and more anthropogenic heat and air pollution than rural areas, which all contribute to the phenomena of urban warming (Arnfield 2003; Cao et al. 2016; Duren and Miller 2012; McCarthy et al. 2010; Oke 1987). However, the exact mechanisms and the relative contributions of different factors of the urban environment to urban climate dynamics are still relatively unknown. Several studies of temperature cycles suggest that there are indeed other climate variables that change independently from the mean temperature during climate change (Qian and Zhang 2015; Stine et al. 2009; Vinnikov et al. 2002; Wang and Dillon 2014). Analyzing the changes in temperature cycles may provide more information regarding the phenomena of urban warming.

Hong Kong has a monsoon-influenced humid subtropical climate. The weather is hot and humid most days of the year, particularly in summer. Less than 25% of the territory's land mass is developed, and Hong Kong is one of the most densely populated cities in the world. The city of Hong Kong has the highest population density and largest volume of buildings. Hong Kong's climate is becoming increasingly warm due to urbanization and climate change (Chan et al. 2012; Li et al. 2015; Siu and Hart 2013), and it is thus considered a good laboratory for urban climate studies. The meteorological station at the headquarters of the Hong Kong Observatory (HKO) began taking hourly observations in the 1880s. The hourly data collected over nearly 130 years

54   provide us with the opportunity to conduct a comprehensive and detailed study of the annual and

55   daily cycles in this highly urbanized city. We hope to determine the extent of the urban effect on

56   different temperature cycles and provide more information on how the urban environment affects

57   the climate.

58   **2   Data and methods**

59   2.1 Hong Kong Observatory hourly air temperature data

60   The hourly meteorological data obtained at four stations in Hong Kong were provided by

61   HKO. The longest observation comes from the HKO station itself, which is located in the city

62   center. Dating back to 1884, the station has been operating for over 130 years, covering the entire

63   period of Hong Kong's growth until it became one of the densest cities in the world. Following a

64   previous study (Siu and Hart, 2013) and the availability of data, another urban station, King's Park

65   (KP), and two rural stations, Ta Ku Ling (TKL) and Tsak Yue Wu (TYW), were also selected. The

66   locations and the satellite images of the surrounding area from Google Earth of the four stations

67   are shown in Fig. 1a. HKO (22°18′07″N, 114 °10′27″E, 32 m above sea level) is located in a

68   compact high-rise area, and 80% of the area around the station is built up. The development of

69   urbanization in this area, as shown from Figure 1b to Figure 1c, provides us with the opportunity

70   to conduct a comprehensive and detailed study of the annual and daily cycles in this highly

71   urbanized city. KP (22°18′43″N, 114 °10′22″E, 65 m above sea level) is located 1 km north of

72   HKO, in a dispersed midrise area, and the surrounding area is 47.4% built up. TKL (22°31′43″N,

73   114 °09′24″E, 15 m above sea level) is located around 25km north of HKO, a dispersed low-rise

74   area with the surrounding area 18.1% built up, and TYW (22°24′11″N, 114 °19′24″E, 5 m above

75   sea level) is a Forest area, around 20 km northeast of HKO, with only a 2.7% built surface around

76   it (Siu and Hart, 2013). Hourly data used in this study date back to 1993, 1989 and 2000 at the KP,

77   TKL and TYW stations, respectively. Note that the HKO data from 1940 to 1946 are not available

78   due to the Second World War. Although there have been changes in the instruments and

79   observations in HKO, the homogeneity test conducted by a previous study showed that the impact

80   of such changes on the temperature homogeneity is negligible (Wong et al 2011).

81   2.2 Fourier Transform

82   We used the Fast Fourier Transform method to convert temperature variation into a set of

83   harmonics. Meteorological temperature data usually form a discrete sequence of N points in time,

84   called a time series. For example, $N = 24 \times 365$ for hourly data over an entire year. The infinite sum

85   can be described by a finite sum, $M = N/2$ harmonics (assuming that N is even), i.e., the discrete

86   Fourier transform. Periodic N-point air temperature variation can be transformed into the sum of

87   harmonics with different frequencies, as follows:

88          $$T(t) = \bar{T} + \sum_{j=1}^{M} \Delta\tilde{T}_j \cos(j\omega t - \Phi_j); \qquad (1)$$

89          $\bar{T}$ is the mean temperature, $\Delta\tilde{T}_j$ is the amplitude and Φ_j is the phase, and $\omega = 2\pi/P$ is the

90   fundamental angular frequency, with the period P for the annual cycle.

91   We focused on the four main harmonics representing the fundamental periodic variation

92   extracted from the complex observed temperature profiles: annual, semi-annual, daily and semi-

93   daily harmonics. The importance of these four harmonics is evident from an example drawn from

94   the observation data obtained at KP in 2000. Fig. 2a shows the amplitude spectrum. The strong

95   signal for the first annual and daily harmonics reflects the primary forcing mechanism, solar

96   radiation. The semi-daily cycle is mainly imposed by the abrupt night-time zeroing of solar

97   radiation in addition to the heat storage of the soil and atmosphere.

98   The observations for an entire year can thus be treated as four periodic variations and other

99   random variations (Fig. 2b), as follows.

100          $$T(t) = \bar{T} + \Delta\tilde{T}_{a1} \cos(\frac{2\pi}{Year}t - \Phi_{a1}) + \Delta\tilde{T}_{a2} \cos(\frac{2\pi}{(Year/2)}t - \Phi_{a2}) + \Delta\tilde{T}_{d1} \cos(\frac{2\pi}{Day}t -$$

101          $$\Phi_{d1}) + \Delta\tilde{T}_{d2} \cos(\frac{2\pi}{(Day/2)}t - \Phi_{d2}) + random(t); \quad (2)$$

102   The major parameters are the mean temperature $\bar{T}$, amplitude $\Delta\tilde{T}_{ai}$ and phase Φ_{ai} of the

103   annual harmonic (12-month harmonic, $i = 1$), semi-annual harmonic (6-month harmonic, $i = 2$),

104   amplitude $\Delta\tilde{T}_{di}$ and phase Φ_{di} daily harmonic (24-hour harmonic, $i = 1$) and the semi-daily cycle

105   (12-hour harmonic, $i = 2$). To gain a better understanding of the phase, we use the peak/bottom

106 temperature occurring time, defined as the phase time in analogy with the phase angle alone, to
107 describe the phase of each harmonic. For annual and daily harmonics, as the peak point is closer
108 to the annual/daily maximum temperature occurring time, the phase time is calculated as the peak
109 temperature occurring time, $\Phi_{a1}/(\frac{2\pi}{Year})$ and $\Phi_{d1}/(\frac{2\pi}{Day})$. For semi-annual and semi-daily
110 harmonics, as the bottom point is closer to the annual/daily minimum temperature occurring time,
111 the phase time is calculated as the first bottom temperature occurring time, $(\Phi_{a2}+\frac{\pi}{2})/(\frac{2\pi}{Year/2})$
112 and $(\Phi_{d2}+\frac{\pi}{2})/(\frac{2\pi}{Day/2})$.

113   The two major harmonics with mean temperature can represent most of the annual and
114 daily variations, as shown in Fig. 2c and Fig. 2d. The root-mean-square error between two-
115 harmonic synthesized and the observed data are 0.5518 and 0.0715 for the annual cycle and daily
116 cycle, respectively. Thus, we obtain the two-harmonic synthesized annual cycle $T_a(t)$ and two-
117 harmonic synthesized daily cycle $T_d(t)$ of each year as follows:

118 $T_a(t) = \bar{T} + \Delta\tilde{T}_{a1}\cos(\frac{2\pi}{Year}t - \Phi_{a1}) + \Delta\tilde{T}_{a2}\cos(\frac{2\pi}{(Year/2)}t - \Phi_{a2}),$　　　(3)

119 $T_d(t) = \bar{T} + \Delta\tilde{T}_{d1}\cos(\frac{2\pi}{Day}t - \Phi_{d1}) + \Delta\tilde{T}_{d2}\cos(\frac{2\pi}{(Day/2)}t - \Phi_{d2}),$　　　(4)

120 According to these two equations, we can then calculate the annual and daily maximum/minimum
121 temperature (*Tx_a, Tn_a, Tx_d, Tn_d*) and their differences in annual temperature range (ATR)
122 and DTR, respectively. The *Tx* and *Tn* are found to be closely related to the amplitudes and mean
123 temperature (*Tm*). *Tx* is the sum of *Tm* with the rise of the amplitudes, and *Tn* is the *Tm* minus the
124 amplitudes. The occurring times of the maximum/minimum temperature for both of the two-
125 harmonic synthesized annual and daily cycles are also calculated ($\Phi_{x\_a}, \Phi_{n\_a}, \Phi_{x\_d}, \Phi_{n\_d}$). The
126 occurring times are associated with the two phases. Note that the annual maximum/minimum
127 temperature and ATR are calculated based on the daily mean temperature to obtain the occurring
128 time change, which is different from traditional definitions where calculations are based on the
129 monthly mean temperature. The differences in annual and daily cycles were compared between
130 urban and rural stations. The long term changes of annual and daily cycles were quantified by
131 linear regression, and the significance of the linear trend was tested by ANOVA F test.

132   **3   Results**

133   3.1 Comparison of the four harmonics and two-harmonic synthesized annual/daily cycles

134   The results from 2014 are selected to compare the differences in the four harmonics and
135   the two-harmonic synthesized annual/daily cycle between the four stations (Fig. 3). The urban
136   stations were found to have larger phase and smaller amplitude for these four harmonics, with a
137   very slight difference in annual and semi-annual harmonics (Fig. 3a, c) and the most evident
138   difference in the daily harmonic (Fig. 3b). The annual amplitude measured at the urban stations
139   was 7.45°C at HKO and 7.43°C at KP, and at the rural stations 7.76°C at TKL and 7.54°C at TYW.
140   The annual phase (days) was 209.5 at HKO; 208.38 at KP; 206.52 at TKL and 204.95 at TYW.
141   The daily amplitudes in the urban stations (HKO 1.30°C and KP 1.59°C) are much smaller than
142   those in the rural stations (TKL 2.77°C and TYW 2.88°C), while the daily phase is much larger in
143   HKO (15.20 hours) than the real rural station TYW (13.52 hours). The daily phase was 14.25 hours
144   at both KP and TKL (Fig. 3b). Similar to the daily harmonic, the semi-daily harmonic showed a
145   significant difference between the four stations, with a much smaller semi-daily amplitude and
146   larger semi-daily phase in the urban stations (Fig. 3d).

147   There are subtle differences in both the annual and semi-annual harmonics between the
148   four stations, while the two-harmonic synthesized annual variations of the air temperature are
149   similar and the urban stations have the higher mean temperature, which suggests that an urban heat
150   island effect existed throughout the whole year (Fig. 3e). However, the two-harmonic synthesized
151   daily cycle variations are entirely different between the four stations. In the urban stations, the
152   daily maximum temperature is cooler, while the daily minimum temperature is much warmer than
153   in the rural stations, resulting in a much smaller DTR. The phase of the daily and semi-daily
154   harmonics demonstrates that the daily maximum and daily minimum temperature appeared much
155   later in the HKO stations (Fig. 3f).

156   Similar results are revealed when the average values from 2000 to 2014 are considered
157   (Table 1; Table 2).

158   3.2 Warming of mean temperature in Hong Kong

159   Hong Kong has experienced a significant warming in air temperature since the late 19th
160   century. Analysis of the mean temperature data from the Hong Kong Observatory showed that
161   there was an average rise of 0.0118°C per year from 1885 to 2014, which is smaller than the long-
162   term warming trend in eastern China for a similar period (Qian 2016), as the observed warming
163   trend is much larger in the higher latitudes (Wang and Dillon 2014). The warming rate being
164   slightly higher than the adjusted warming trend after de-urbanization in eastern China (Qian 2016)
165   and the globally averaged 0.85°C per-century warming for a similar period (IPCC 2013) suggest
166   that global warming and the local urbanization effect may both contribute to the urban warming
167   of Hong Kong. From the 1880s to the 1960s, the warming trend was slight, while dramatic
168   warming occurred between the 1980s and the 2000s. The temperature showed decreasing trends
169   in two periods, from the 1960s to the 1980s and from the 2000s to the present. The other urban
170   station, KP, only presents the same decadal change of mean temperature from the 1990s due to
171   data availability, while the temperature was consistently 0.3°C cooler than at HKO. The two rural
172   stations show different characteristics of mean temperature variation, and both were more than
173   1°C cooler than the HKO urban stations (Table 1, Fig. 4). We compared the annual mean
174   temperature data for HKO and TKL for the same period of 1989 to 2014 and found the warming
175   rate experienced by HKO (0.0082 °C per year) to be twice that of TKL (0.0045 °C per year). Thus,
176   the local urban effect could be estimated to contribute 50% of the warming of the air temperature
177   in the urban area of Hong Kong from 1989 to 2014. As the HKO station trend reversed to show a
178   decrease after 2000, the TYW station also showed a cooling trend from 2000-2014.

179   3.3 Changes in amplitude and phase of the four harmonics

180   For the annual harmonic, two main phenomena can be identified. First, all four stations
181   show negligible differences in annual and semi-annual harmonics. The differences between the
182   four stations are too small to be distinguished from the figures (Fig. 5). The Pearson correlation
183   coefficients of the four stations are significantly positive. For example, the four stations appear to
184   have experienced similar variations for the annual phase through the simultaneous observations
185   (Table 4). Second, no obvious trend in the changes of the amplitudes in the urban station HKO is
186   observed over the past 130 years, either in annual amplitude (-0.0018°C/year, P value 0.0796) or

187　semi-annual amplitude (0.0006C/year, P value 0.4918). The phases show decreasing trends

188　(annual phase: -0.0244 days/year, P value 0.0095, semi-annual phase: -0.0672 days/year, P value

189　0.0325).

190　　　　The changes in the daily amplitudes and phases show totally different characteristics from

191　those in the annual amplitudes and phases. For daily and semi-daily harmonics, significant

192　discrepancies are found between the urban and rural stations. Taking the daily phase as an example,

193　the calculated correlation coefficients between the four stations are all extremely small, and

194　negative values even occur. The largest positive correlation appears between the two rural stations

195　and is significant at a 0.05 level.

196　　　　The daily amplitude in the urban stations is much smaller than in rural stations, while the

197　phase is much larger. Over the past 130 years, the amplitude change in HKO data can be divided

198　into three periods. Before the 1960s, the amplitude showed a slightly increasing trend. From the

199　1960s to the 1990s, the trend began to dramatically decrease. After the 2000s, the amplitude

200　leveled off. Due to the lack of data, the long-term change in amplitude of the rural stations could

201　not be discovered. However, the amplitude and the decadal change appear to be approximately

202　similar in the two rural stations.

203　　　　In addition to the amplitude change, the difference in the changes in the daily phase

204　between urban and rural stations is remarkable. The daily phase in the urban areas is more than

205　one hour later than in the rural areas. What is striking is the clear growth trend in the time lag

206　between the daily maximum air temperature and solar radiation, which amounts to a delay of over

207　1.5 hours during the past 130 years (0.0136 hours per year, significant at 0.01 level). Such a delay

208　of phase lag has not been previously reported. No clear trend in the change in the phase of the daily

209　air temperature cycle in other rural stations can be identified. The delay of the phase was unique,

210　only occurring in urban areas. Interestingly, the daily phase at the rural station TYW in the 2000s

211　is close to those taken at HKO in the late 1890s, when Hong Kong was just a village.

212　　　　The changes in the amplitudes and phase of the semi-daily harmonic show similar

213　characteristics to the daily harmonic except for the semi-daily phase. First, the difference in the

214　semi-daily phase between urban and rural is much smaller than that of the daily phase. The semi-

215   daily phase of HKO shows a continuous trend of delay over the past 130 years, which is also

216   different from that of the daily phase.

217   3.4 Changes in annual and daily maximum/minimum temperatures

218   The urban stations have a higher mean temperature and slightly smaller amplitude and

219   exhibit higher annual maximum and minimum temperatures than the rural stations (Table 2; Fig.

220   7). The difference between urban and rural stations is larger in terms of minimum temperature.

221   Thus, the ATR is slightly smaller in the urban stations. However, the urban-rural difference in the

222   daily pattern is totally different from the annual pattern. The urban daily maximum temperature is

223   cooler than the rural daily maximum, while the urban daily minimum temperature is much warmer.

224   The DTR is dramatically smaller in the urban area. Taking 2000-2014 average data of HKO and

225   TYW as an example, their difference in annual maximum temperature is 1°C, while their

226   difference in annual minimum temperature is 1.8°C. The ATR in HKO is 0.79°C smaller than that

227   in TYW. The daily maximum temperature in HKO is 0.88°C cooler than TYW, while the daily

228   minimum temperature is 2.39°C warmer. Thus, the DTR in HKO station is less than half of that in

229   TYW (2.92°C to 6.19°C) (Table 2).

230   For the last 130 years, the warming trends of the annual maximum and annual minimum

231   temperatures are comparable, at 0.0105°C per year and 0.0136°C per year. Both are significant at

232   the 0.01 level and very similar to the trend of the mean temperature. Thus, ATR showed a very

233   slightly decreasing trend (-0.0031°C per year, P value 0.1391). Fig. 7 illustrates that the annual

234   maximum and minimum temperatures have not shown any obvious break or abruption over the

235   time period. The linear trends of the daily maximum and minimum temperatures for the whole

236   period between 1885 and 2014 are comparable (0.0123°C and 0.0105°C per year), and the DTR

237   changed increased very subtly over 130 years (0.0018°C per year). However, the daily maximum

238   and minimum temperatures also showed discontinuities (Fig. 7), as both daily amplitudes

239   experienced discontinuous variations (Fig. 6). The changes of daily maximum and minimum

240   temperatures and DTR must be examined in three different periods (Table 6). From 1885 to 1959,

241   the daily maximum temperature increased much faster than daily minimum temperature, resulting

242   in the increasing DTR. From 1960 to 1999, the daily maximum temperature started to show a

243   decreasing trend, while the daily minimum temperature showed an even larger warming trend

244 compared to the former period, producing a significant decreasing trend of DTR during this period.

245 After 2000, abruptions then occurred, and the daily maximum and minimum temperatures and

246 DTR all reversed from the former period. The daily maximum temperature increased while the

247 daily minimum temperature decreased, generated the increasing DTR.

248 3.5 Variations in the occurring times of maximum and minimum temperatures

249 Our analysis of the four harmonics demonstrates that the diversity in the annual phase is

250 much smaller than in the daily phase between the four stations. Closely related to the phases, the

251 differences in the occurring times of annual maximum and minimum temperatures are smaller than

252 in the occurring times of the daily maximum and minimum temperatures between different stations

253 (Fig. 8; Table 2).

254 In the HKO stations, both the annual phase and the semi-annual phase showed decreasing

255 trends over the 130-year period. However, the annual warmest time and coolest time moved in the

256 opposite direction. The annual warmest time was delayed (0.0466 days per year, P value 0.1257),

257 while the annual coolest time appeared earlier (-0.0575 days per year, P value 0.0002). In contrast,

258 both the daily phase and the semi-daily phase showed increasing trends over the 130 years at HKO.

259 The daily warmest and coolest times were both delayed, as the two phases show. The daily coolest

260 time delayed with a trend of 0.0125 hour per year (P value 0), which is larger than the 0.0107 (P

261 value 0) hour per year for the daily warmest time. The main difference between the daily warmest

262 and coolest times appeared after 2000, when the daily warmest time reversed to show a decreasing

263 trend and the daily coolest time continued to show a delaying trend (Fig. 8).

264 **4   Discussion and conclusions**

265 Different temperature cycles are associated with different spatial scales (Mitchell 1976).

266 Our results show that the difference in annual cycles between urban and rural stations is much

267 smaller than that in daily cycles, suggesting that the urban area has a greater effect on daily cycles

268 than on annual cycles. Studies have demonstrated that the factors affecting the annual cycle range

269 from regional to global; these include latitude, altitude, distance to the ocean, greenhouse-gas

270 forcing and atmospheric circulation (Cornes et al. 2017; McKinnon et al. 2013; Prescott and

271 Collins 1951; Qian and Zhang 2015; Stine and Huybers 2012; Stine et al. 2009). The similar

272   variations in the annual cycles of the four stations in Hong Kong indicate that urban areas have
273   very little impact on the annual cycle. The change in annual cycles may be a large-scale
274   phenomenon. The decreased annual amplitudes and ATR suggest a larger warming trend in winter
275   than in summer, which has been revealed by observations (Balling Jr et al. 1998; Luterbacher et
276   al. 2004; Stine et al. 2009), reanalysis (Cornes et al. 2017), and CMIP5 models (Qian and Zhang
277   2015). Qian and Zhang (2015) analyzed the observation and CMIP5 model outputs to study the
278   contributions of different nature and anthropogenic forcing to the observed decreasing annual
279   amplitude and suggested that the prominent signal on changes in the annual temperature cycle only
280   from the greenhouse gas effect and land use change seems to contribute little. As the major factor
281   accompanying the urbanization effect on urban climate is the land use/cover change, the observed
282   similar annual patterns of air temperature between urban and rural stations in this study also
283   suggest that the land use/cover change contribute little to the annual cycle. The long-term change
284   in annual phases in HKO data also confirmed findings in the analysis of annual phase or change
285   of seasons that revealed a shift in the annual phase (Stine et al. 2009) and the earlier onset of
286   seasons (Cassou and Cattiaux 2016; Cayan et al. 2001), which are also consistent with the annual
287   coolest time in HKO occurring significantly earlier. However, the delayed annual warmest time
288   has not been previously reported. The exact mechanism of the annual coolest and warmest times
289   requires further study.

290   Unlike annual cycles, the difference in daily cycles between urban and rural stations is
291   distinct, which implies that the daily cycle is more appropriate to indicate urban local climate
292   change. In the urban area of Hong Kong, the daily maximum temperature is smaller, while the
293   minimum temperature is much larger, so the DTR in the urban area is dramatically smaller. The
294   daily phases or daily warmest and coolest times all occur much later in the urban area. The
295   characteristics in amplitudes (DTR) and phases (or warmest and coolest time) can be mainly
296   ascribed to thermal storage. The smaller daily amplitudes and DTR may be associated with
297   increased thermal storage in the urban area. Yang et al. (2017) suggested that the thermal storage
298   of the urban area is the main force behind the urban cool island clearly observed in Hong Kong.
299   The larger thermal storage dampens the urban surface temperature, making it and the air
300   temperature cooler in the daytime. This explanation is related to the phenomenon of the urban heat
301   sink, where the city surface temperature is cooler than the surrounding area (Carnahan and Larson
302   1990; Giannaros et al. 2013). The strong night-time urban heat island may be due to the

303 combination effect of urban thermal storage and anthropogenic heat. Another phenomenon of
304 concern is that the daily and semi-daily phases and daily warmest and coolest times are all delayed.
305 Kuo (1968) developed a radiative conductive atmospheric boundary layer model to study the
306 thermal interaction between the atmosphere and the underlying ground, related to diurnal solar
307 radiative heating. The results showed that the phase lag of the near surface potential temperature
308 cycle is determined by the effective heat capacities of the atmosphere and the surface. Wang et al.
309 (2017) developed a conceptual energy balance model to study the urban temperature cycle. The
310 analytical solution suggested that the changes in amplitude and phase are independent from the
311 mean temperature. The amplitude and phase are mainly determined by the effective thermal
312 storage. Therefore, the increasing number of human-made structures in the urban area, such as
313 buildings and roads, which have low reflectivity and high thermal capacity, have increased the
314 thermal storage of the cities. A delayed daily phase and occurring time of the daily maximum and
315 minimum temperatures can thus be expected.

316   However, the daily amplitudes (DTR) and phases (or warmest and coolest time) in HKO
317 did not show consistent decreasing or delaying phenomena during the study period. The long-term
318 daily amplitudes and DTR showed discontinuities over the past 130 years: they experienced an
319 increasing trend before the 1960s, then decreased from the 1960s to the 1990s, then reversed again
320 to show an increasing trend after 2000. The reversed trend of the DTR after the 1990s were also
321 reported in China (Qian et al 2011; Wang et al 2012). The long-term observations were consistent
322 with the long-term variation of the DTR reported for most areas of the world (Thorne et al. 2016a;
323 Thorne et al. 2016b; Wild 2009). Although we found a significant delaying of the phases and
324 timings of daily maximum and minimum temperatures, the phase delay mainly occurred before
325 the 1910s and from the 1940s to the 1990s. There was a surprising phase advance phenomenon,
326 i.e., a significant daily phase advance and daily warmest time, earlier in HKO, during the 1910s-
327 1940s and the 2000s. As far as we are aware, these phase delay and advance phenomena have not
328 been previously reported or explained. We suggest that the thermal storage increase is the main
329 influencing parameter for the observed phase delay phenomenon. However, the observed
330 significant phase advance phenomenon suggests that changes in solar radiation and the effect of
331 air pollution (through its effect on solar radiation) are significant, but their exact mechanisms are
332 at present unknown. The phase delay and advance in the different periods coincide with the
333 dimming and brightening in global solar radiation (Wild 2009), which suggests that the daily

334 temperature cycle is also closely related to larger-scale climate factors. The understanding of the
335 nonlinear multi-decadal variations in daily temperature cycles may help us identify any
336 relationship between global warming and urban warming, and perhaps in particular the effect of
337 global warming on urban warming. Such variations in daily cycles of HKO also suggested that,
338 other than simple linear trends, the nonlinear approaches may be more accurate in describing the
339 multi decadal variations (Qian 2016; Wu et al 2007).

346 **References**

347 Arnfield AJ (2003) Two decades of urban climate research: a review of turbulence, exchanges of
348   energy and water, and the urban heat island International Journal of Climatology 23:1-26

349 Balling Jr RC, Michaels PJ, Knappenberger PC (1998) Analysis of winter and summer warming
350   rates in gridded temperature time series Climate Research 9:175-181

351 Cao C, Lee X, Liu S, Schultz N, Xiao W, Zhang M, Zhao L (2016) Urban heat islands in China
352   enhanced by haze pollution Nature Communications 7:12509 doi:10.1038/ncomms12509

353 Carnahan WH, Larson RC (1990) An analysis of an urban heat sink Remote Sensing of
354   Environment 33:65-71

355 Cassou C, Cattiaux J (2016) Disruption of the European climate seasonal clock in a warming world
356   Nature Climate Change 6:589-594

357 Cayan DR, Dettinger MD, Kammerdiener SA, Caprio JM, Peterson DH (2001) Changes in the
358   onset of spring in the western United States Bulletin of the American Meteorological
359   Society 82:399-415

360 Chan H, Kok M, Lee T (2012) Temperature trends in Hong Kong from a seasonal perspective
361   Climate Research 55:53-63

362 Cornes RC, Jones P, Qian C (2017) Twentieth-century trends in the annual cycle of temperature
363   across the northern hemisphere Journal of Climate, doi:10.1175/JCLI-D-16-0315.1

364   Duren RM, Miller CE (2012) Measuring the carbon emissions of megacities Nature Climate
365   Change 2:560-562

366   Easterling DR et al. (1997) Maximum and minimum temperature trends for the globe Science
367   277:364-367

368   Gallo KP, Easterling DR, Peterson TC (1996) The influence of land use/land cover on
369   climatological values of the diurnal temperature range Journal of Climate 9:2941-2944

370   Giannaros TM, Melas D, Daglis IA, Keramitsoglou I, Kourtidis K (2013) Numerical study of the
371   urban heat island over Athens (Greece) with the WRF model Atmospheric Environment
372   73:103-111

373   IPCC (2013) Climate Change 2013: The Physical Science Basis. Contribution of Working Group
374   I to the Fifth Assessment Report of the Intergovernmental Panel on Climate Change.
375   Cambridge University Press, Cambridge, United Kingdom and New York, NY, USA.
376   doi:10.1017/CBO9781107415324

377   Jones PD, Groisman PY, Coughlan M, Plummer N, Wang WC, Karl TR (1990) Assessment of
378   urbanization effects in time series of surface air temperature over land Nature 347:169-172

379   Kuo HL (1968) The thermal interaction between the atmosphere and the earth and propagation of
380   diurnal temperature waves Journal of the Atmospheric Sciences 25:682-717

381   Li L, Chan PW, Wang D, Tan M (2015) Rapid urbanization effect on local climate:
382   intercomparison of climate trends in Shenzhen and Hong Kong, 1968-2013 Climate
383   Research 63:145-155

384   Luterbacher J, Dietrich D, Xoplaki E, Grosjean M, Wanner H (2004) European seasonal and
385   annual temperature variability, trends, and extremes since 1500 Science 303:1499-1503

386   McCarthy MP, Best MJ, Betts RA (2010) Climate change in cities due to global warming and
387   urban effects Geophysical Research Letters 37, L09705, doi:10.1029/2010GL042845

388   McKinnon KA, Stine AR, Huybers P (2013) The spatial structure of the annual cycle in surface
389   temperature: Amplitude, phase, and Lagrangian history Journal of Climate 26:7852-7862

390   Mitchell JM (1976) An overview of climatic variability and its causal mechanisms Quaternary
391   Research 6:481-493

392   Oke TR (1987) Boundary layer climates. 2nd. Routledge

393   Prescott JA, Collins JA (1951) The lag of temperature behind solar radiation Quarterly Journal of
394   the Royal Meteorological Society 77:121-126

395   Qian C. (2016) Disentangling the urbanization effect, multi-decadal variability, and secular trend
396   in temperature in eastern China during 1909-2010 Atmospheric Science Letters 17:177-
397   182

398   Qian C, Fu C, Wu Z (2011) Changes in the amplitude of the temperature annual cycle in China
399   and their implication for climate change research Journal of Climate 24:5292-302

400   Qian, C, Zhang X. (2015) Human influences on changes in the temperature seasonality in mid-to
401   high-latitude land areas Journal of Climate 28:5908-5921

402   Siu LW, Hart MA (2013) Quantifying urban heat island intensity in Hong Kong SAR, China
403   Environmental monitoring and assessment 185:4383-4398

404   Stine AR, Huybers P (2012) Changes in the seasonal cycle of temperature and atmospheric
405   circulation Journal of Climate 25:7362-7380

406   Stine AR, Huybers P, Fung IY (2009) Changes in the phase of the annual cycle of surface
407   temperature Nature 457:435-440

408   Thorne P et al. (2016a) Reassessing changes in diurnal temperature range: Intercomparison and
409   evaluation of existing global data set estimates Journal of Geophysical Research:
410   Atmospheres 121:5138-5158

411   Thorne P et al. (2016b) Reassessing changes in diurnal temperature range: A new data set and
412   characterization of data biases Journal of Geophysical Research: Atmospheres 121:5115-
413   5137

414   Vinnikov KY, Robock A, Basist A (2002) Diurnal and seasonal cycles of trends of surface air
415   temperature Journal of Geophysical Research: Atmospheres 107

416   Wang G, Dillon ME (2014) Recent geographic convergence in diurnal and annual temperature
417   cycling flattens global thermal profiles Nature Climate Change 4:988-992

418   Wang K, Ye H, Chen F, Xiong Y, Wang C (2012) Urbanization effect on the diurnal temperature
419   range: different roles under solar dimming and brightening Journal of Climate 25:1022-
420   1027

421   Wang K, Li Y, Wang Y, Yang X (2017) On the asymmetry of the urban daily air temperature cycle
422   Journal of Geophysical Research: Atmospheres 122, doi:10.1002/2017JD026589.

423   Wild M (2009) Global dimming and brightening: a review Journal of Geophysical Research:
424   Atmospheres 114

425   Wong MC, Mok HY, Lee TC (2011) Observed changes in extreme weather indices in Hong Kong
426   International Journal of Climatology 31:2300-2311

427   Wu Z, Huang NE, Long SR, Peng CK (2007) On the trend, detrending, and variability of nonlinear
428   and nonstationary time series Proceedings of the National Academy of Sciences 104:
429   14889-14894.

430   Yang X, Li Y, Luo Z, Chan PW (2017) The urban cool island phenomenon in a high-rise high-
431   density city and its mechanisms International Journal of Climatology 37: 890-904
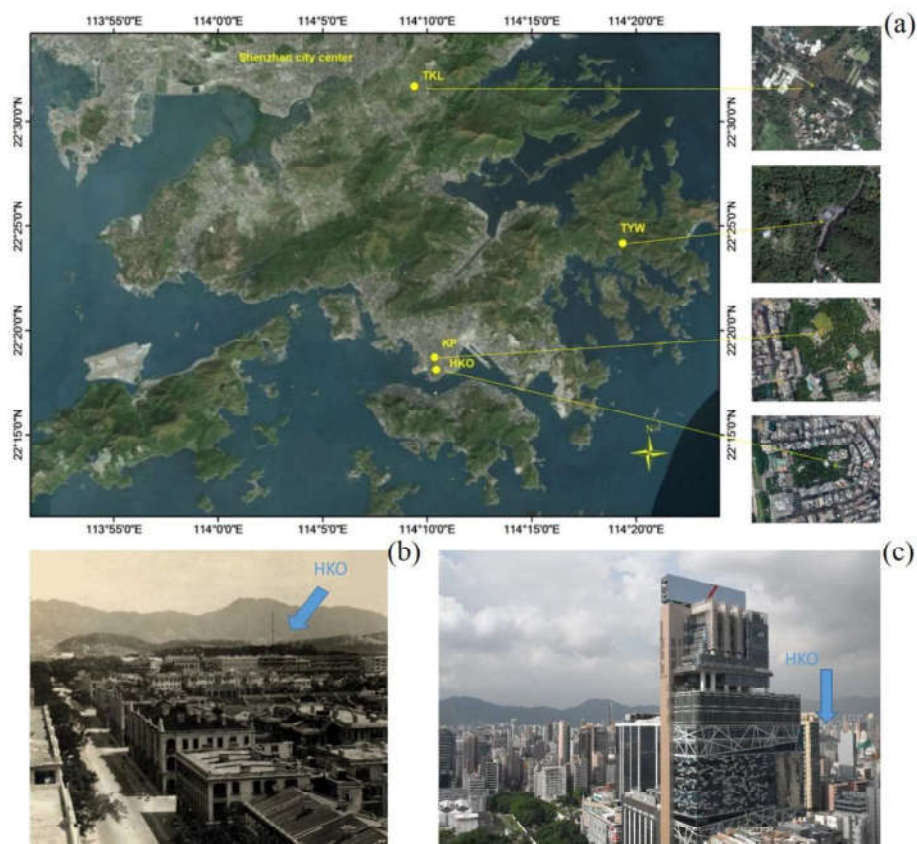
432   **Figure Captions**

433   Fig. 1 Locations of four selected meteorological stations in Hong Kong (a) and illustration of the
434   urban development around HKO stations from 1920s (b) to 2017 (c). (Figure 1b courtesy of Mr.
435   Shun Chi-ming)

436   Fig. 2 Discrete Fourier transform of sample data: (a) energy spectrum showing four major
437   harmonics in observed hourly data (meteorological station KP in 2000); (b) comparison of annual
438   hourly observed data and sum of four major harmonics; (c) comparison of monthly observed mean
439   temperature in 2000, annual harmonic and sum of annual and semi-annual harmonics; and (d)
440   comparison of observed average hourly mean in 2000, daily harmonic of observed average hourly
441   mean in 2000 and sum of daily and semi-daily harmonics.

442   Fig. 3 Comparison of the four major harmonics: the annual harmonic (a), daily harmonic (b), semi-
443   annual harmonic (c), and semi-daily harmonic (d) of the four selected stations in 2014. (e) and (f)
444   are the two-harmonic synthesized annual cycle and two-harmonic synthesized daily cycle,
445   respectively, which are calculated from the sum of two harmonics with mean temperature. Dashed
446   lines in these two figures denote the mean temperatures of the four stations.

447   Fig. 4 Change in the mean temperature at stations in Hong Kong.

448   Fig. 5 Changes in the annual and semi-annual harmonics in Hong Kong: (a) annual amplitude; (b)
449   annual phase; (c) semi-annual amplitude; (d) semi-annual phase. JDN is Julian day number.

450   Fig. 6 Changes in the daily harmonic and semi-daily harmonic in Hong Kong: (a) daily amplitude;
451   (b) daily phase; (c) semi-daily amplitude; (d) semi-daily phase. LST is local solar time.

452   Fig. 7 Changes in the two-harmonic synthesized annual and daily temperature cycles in Hong
453   Kong: (a) annual maximum temperature; (b) daily maximum temperature; (c) annual minimum
454   temperature; (d) daily minimum temperature; (e) annual temperature range; (f) diurnal temperature
455   range.

456   Fig. 8 Changes in the occurring times of annual maximum (a), annual minimum (c), daily
457   maximum (b) and daily minimum (d) temperatures. JDN is Julian day number, LST is local solar
458   time.

459 **Table Captions**

460 Table 1 2000-2014 averages of the mean temperature (°C), amplitude (°C) and phase (day or hour)
461 of the four harmonics.

462 Table 2 The 2000-2014 averages of annual and daily maximum, minimum temperatures and
463 temperature ranges (°C) in the four stations, and their occurring times (Julian day number or local
464 solar time), all calculated from two-harmonic synthesized annual and daily cycles.

465 Table 3 Linear trend in measurements taken at four Hong Kong meteorological stations.

466 Table 4 Pearson correlation coefficients of annual phase between four stations.

467 Table 5 Pearson correlation coefficients of the daily phase between the four stations.

468 Table 6 Linear trends (°C per year) of the daily maximum temperature (Tx_d), daily minimum
469 temperature (Tn_d) and DTR for different periods in HKO.

470

Fig. 1 Locations of four selected meteorological stations in Hong Kong (a) and illustration of the urban development around HKO stations from 1920s (b) to 2017 (c). (Figure 1b courtesy of Mr. Shun Chi-ming)
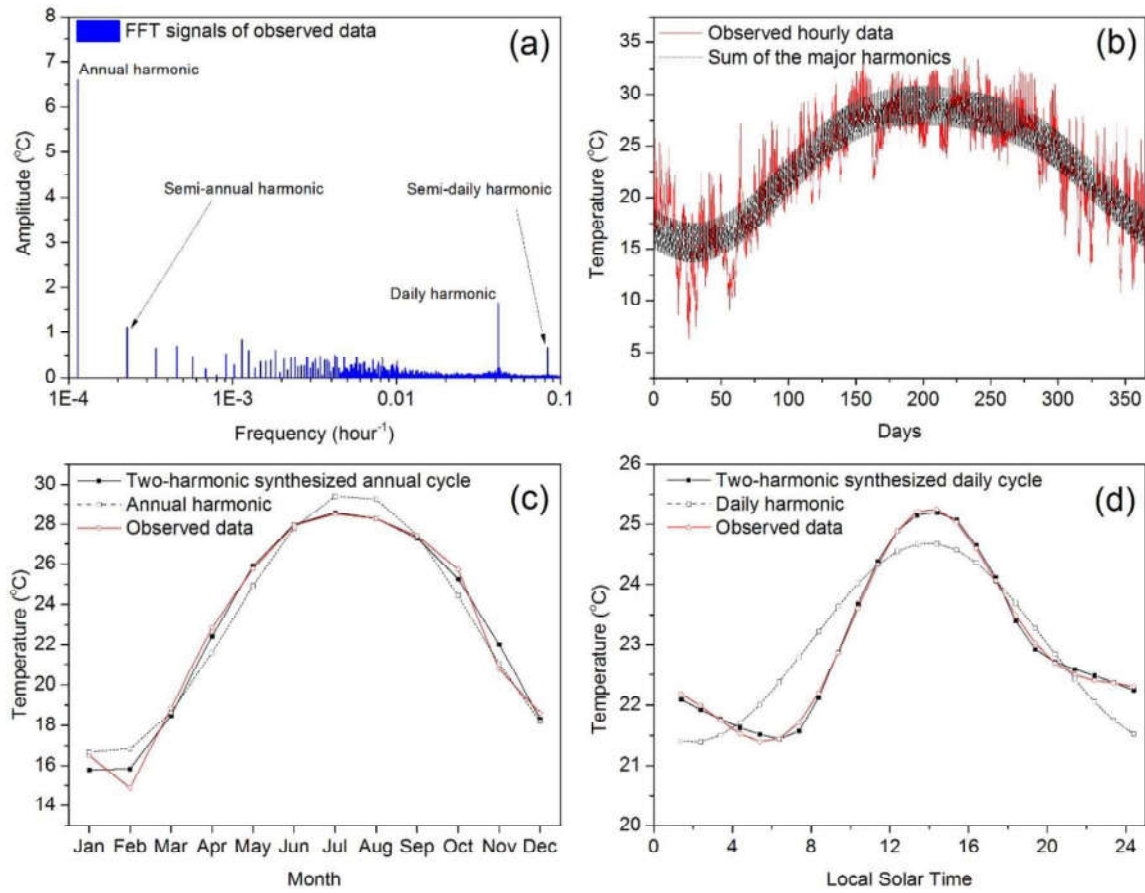
Fig. 2 Discrete Fourier transform of sample data: (a) energy spectrum showing four major harmonics in observed hourly data (meteorological station KP in 2000); (b) comparison of annual hourly observed data and sum of four major harmonics; (c) comparison of monthly observed mean temperature in 2000, annual harmonic and sum of annual and semi-annual harmonics; and (d) comparison of observed average hourly mean in 2000, daily harmonic of observed average hourly mean in 2000 and sum of daily and semi-daily harmonics.
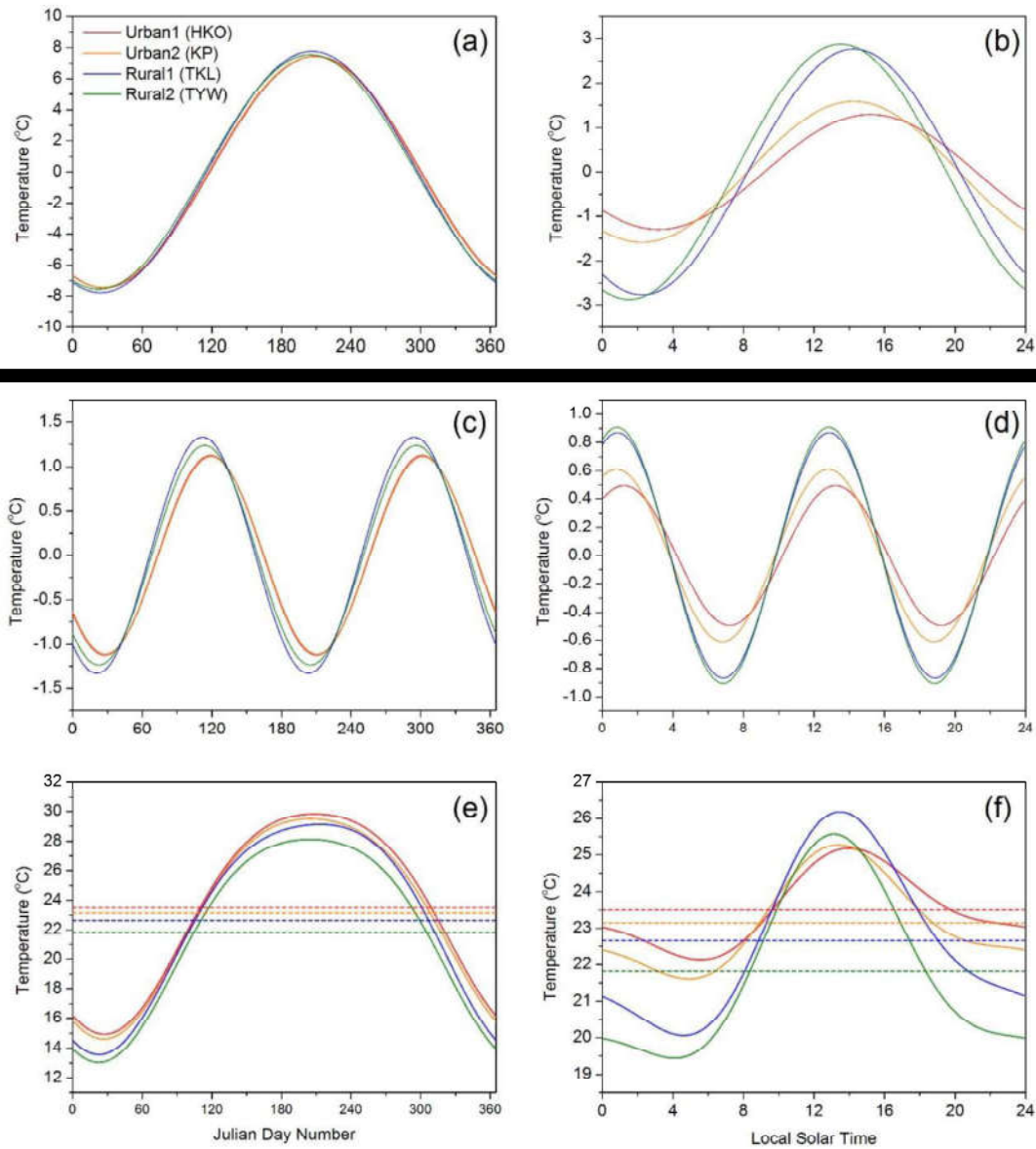
Fig. 3 Comparison of the four major harmonics: the annual harmonic (a), daily harmonic (b), semi-annual harmonic (c), and semi-daily harmonic (d) of the four selected stations in 2014. (e) and (f) are the two-harmonic synthesized annual cycle and two-harmonic synthesized daily cycle, respectively, which are calculated from the sum of two harmonics with mean temperature. Dashed lines in these two figures denote the mean temperatures of the four stations.
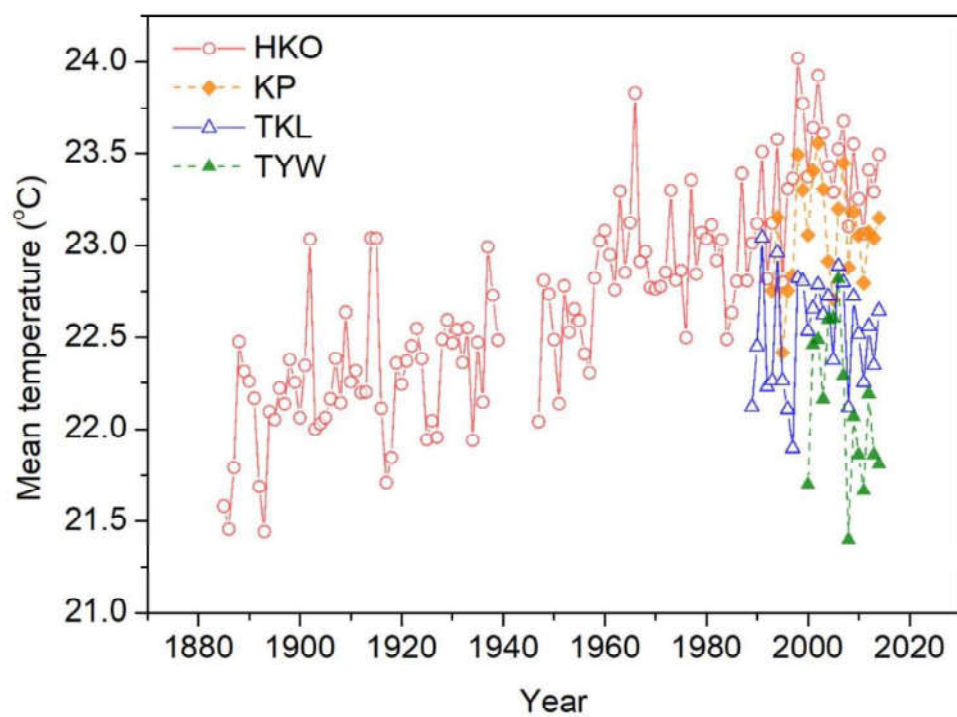
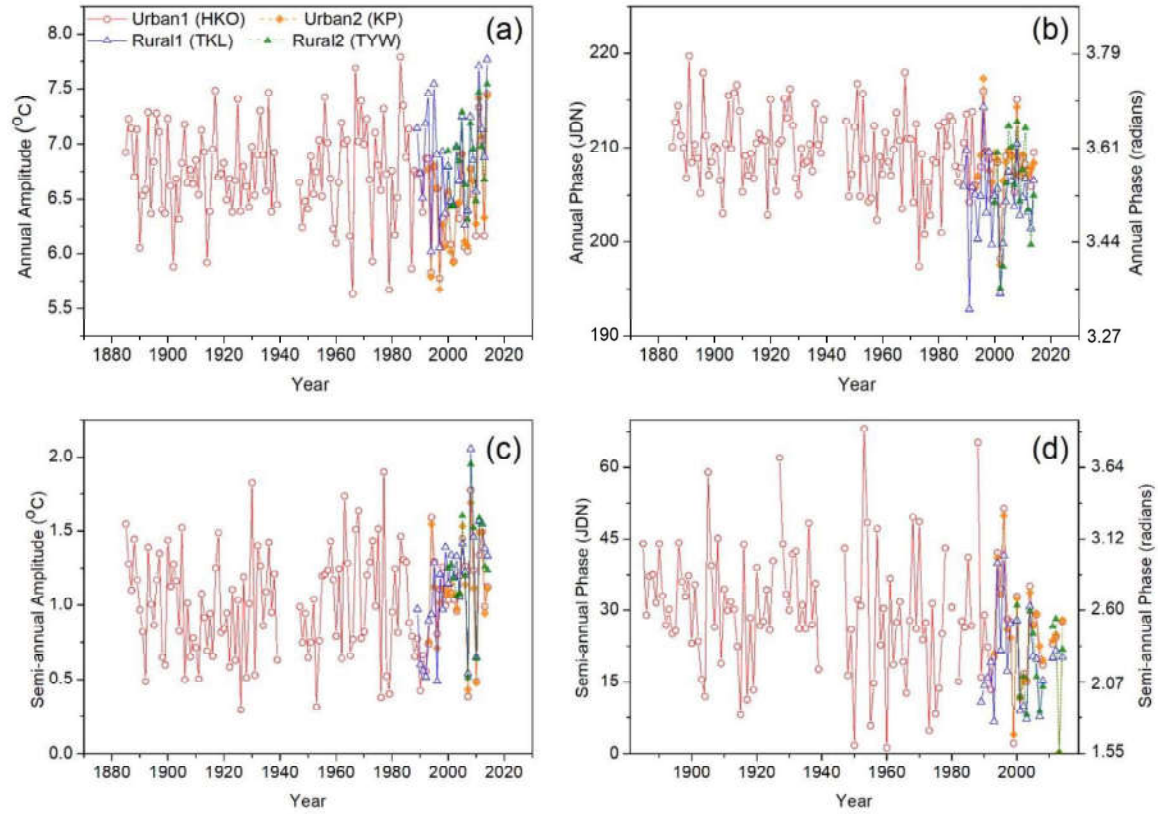Fig. 4 Change in the mean temperature at stations in Hong Kong.

Fig. 5 Changes in the annual and semi-annual harmonics in Hong Kong: (a) annual amplitude; (b) annual phase; (c) semi-annual amplitude; (d) semi-annual phase. JDN is Julian day number.
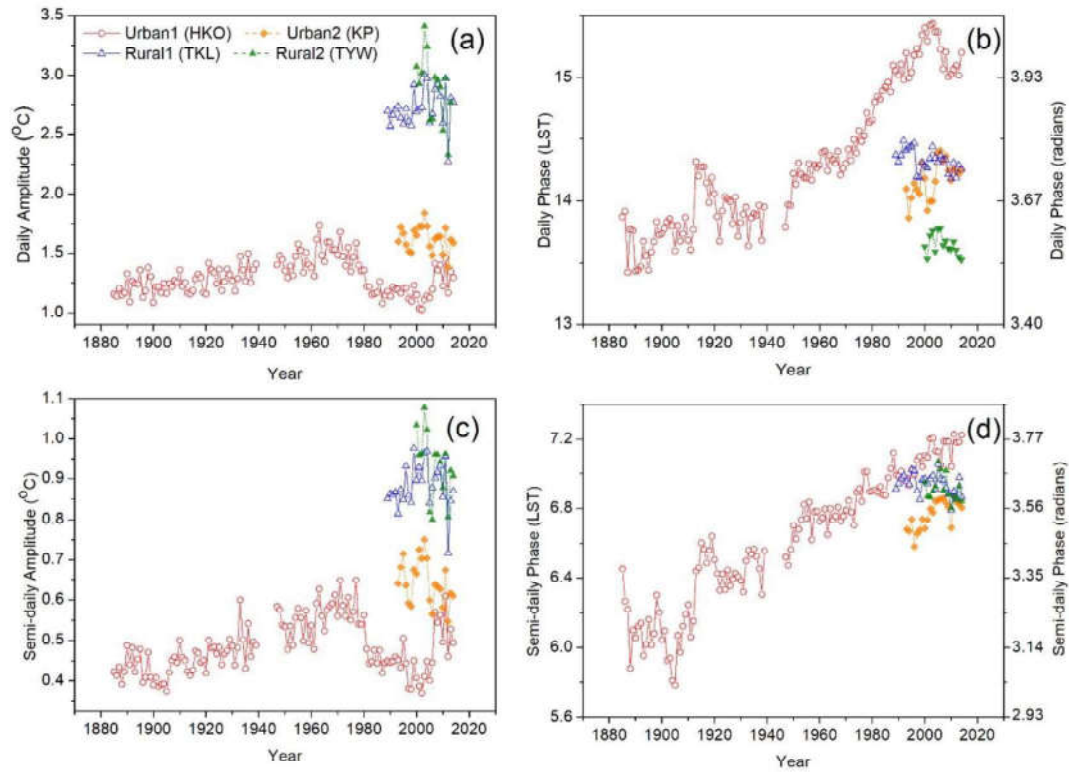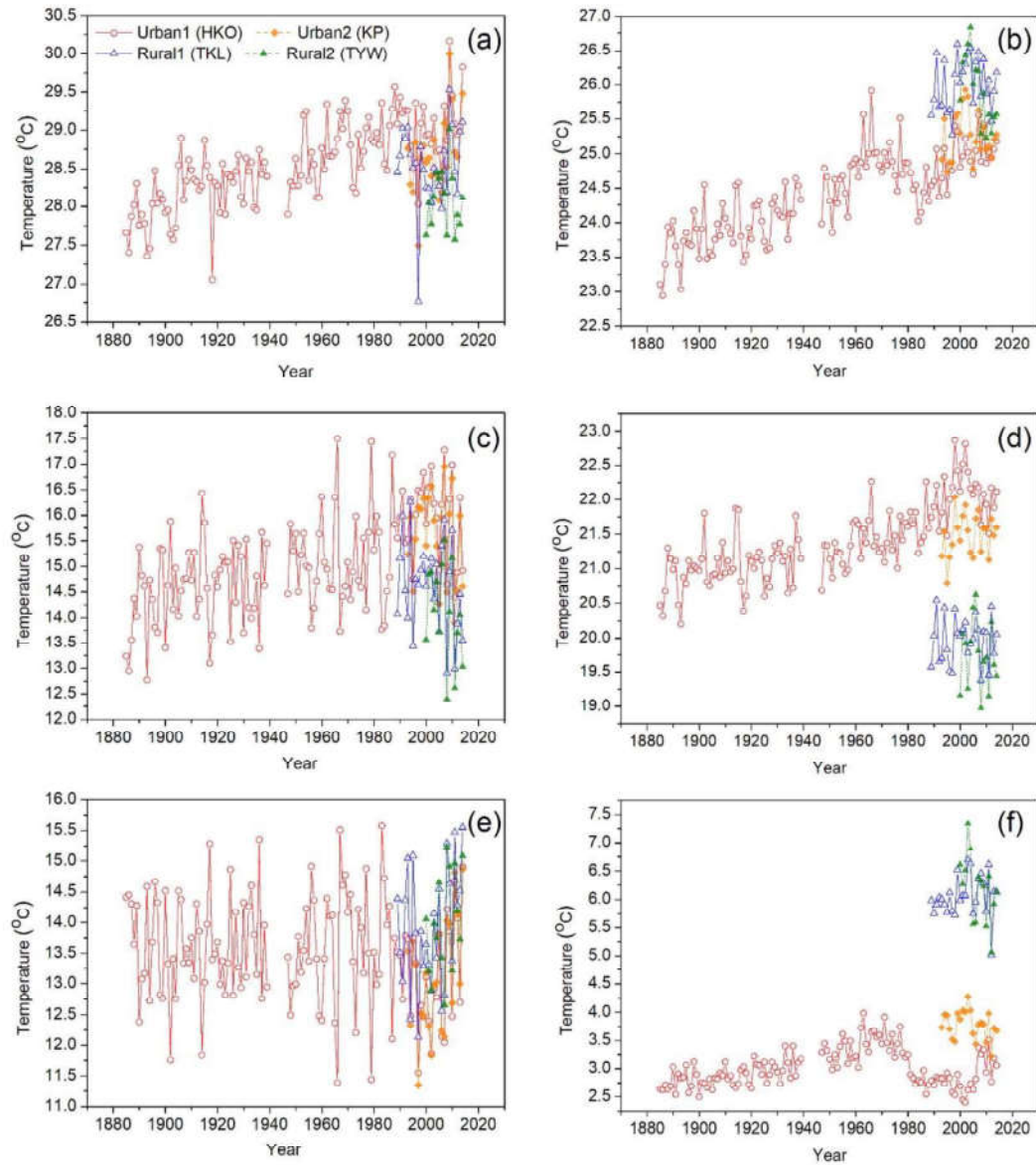
Fig. 6 Changes in the daily harmonic and semi-daily harmonic in Hong Kong: (a) daily amplitude; (b) daily phase; (c) semi-daily amplitude; (d) semi-daily phase. LST is local solar time.

Fig. 7 Changes in the two-harmonic synthesized annual and daily temperature cycles in Hong Kong: (a) annual maximum temperature; (b) daily maximum temperature; (c) annual minimum temperature; (d) daily minimum temperature; (e) annual temperature range; (f) diurnal temperature range.
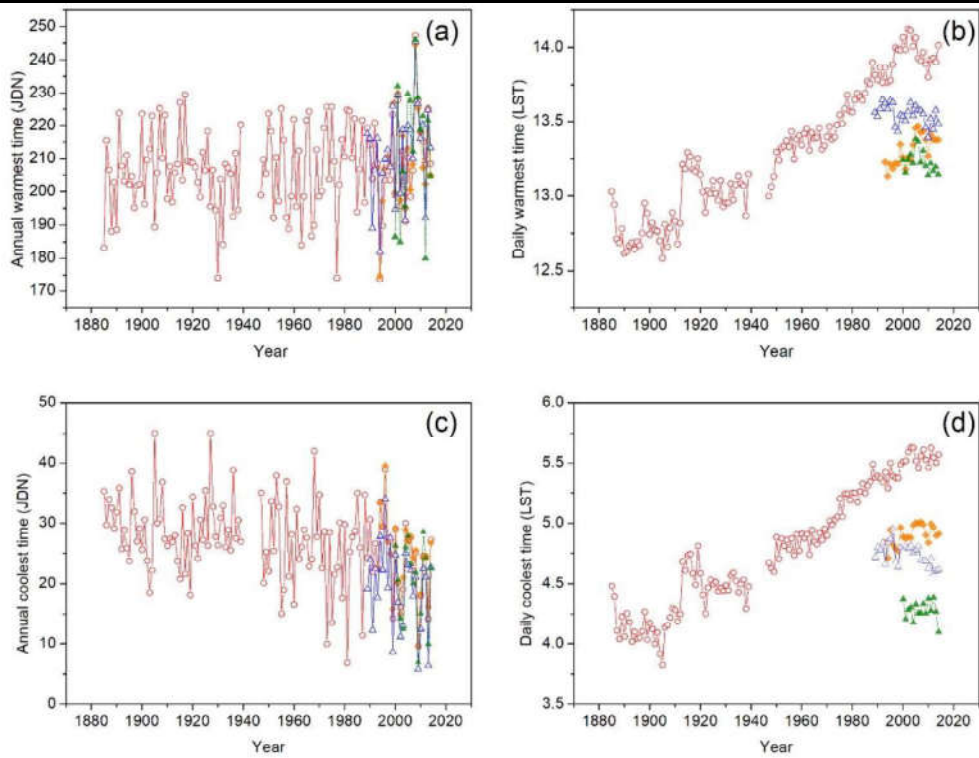
Fig. 8 Changes in the occurring times of annual maximum (a), annual minimum (c), daily maximum (b) and daily minimum (d) temperatures. JDN is Julian day number, LST is local solar time.

Tables

Table 1 2000-2014 averages of the mean temperature (°C), amplitude (°C) and phase (day or hour) of the four harmonics.

Parameters		HKO	KP	TKL	TYW
Mean	T_m	23.44 $\pm$ 0.23	23.12 $\pm$ 0.24	22.57 $\pm$ 0.22	22.13 $\pm$ 0.41
Annual	$\Delta\tilde{T}_{a1}$	6.52±0.49	6.56±0.48	6.89±0.46	6.87±0.38
	Φ_{a1}	207.66±3.62	207.84±3.41	204.18±3.73	205.70±5.34
Semi-annual	$\Delta\tilde{T}_{a2}$	1.12±0.35	1.12±0.35	1.28±0.36	1.26±0.37
	Φ_{a2}	23.44±7.25	21.97±9.40	17.73±7.82	18.95±9.85
Daily	$\Delta\tilde{T}_{d1}$	1.23±0.14	1.63±0.12	2.76±0.19	2.88±0.28
	Φ_{d1}	15.21±0.16	14.21±0.14	14.30±0.07	13.64±0.08
Semi-daily	$\Delta\tilde{T}_{d2}$	0.48±0.07	0.64±0.06	0.89±0.06	0.93±0.08
	Φ_{d2}	7.16±0.06	6.80±0.06	6.93±0.06	6.91±0.07

Table 2 The 2000-2014 averages of annual and daily maximum, minimum temperatures and temperature ranges (°C) in the four stations, and their occurring times (Julian day number or local solar time), all calculated from two-harmonic synthesized annual and daily cycles.

Parameters		HKO	KP	TKL	TYW
Annual maximum	Tx_a	29.09±0.45	28.80±0.52	28.53±0.45	28.09±0.40
	Φ_{x_a}	212.71±14.77	212.53±14.02	214.69±15.19	213.14±19.62
Annual minimum	Tn_a	15.89±0.92	15.54±0.97	14.50±0.93	14.09±0.94
	Φ_{n_a}	22.31±5.96	22.57±5.71	17.73±6.45	20.00±6.73
ATR		13.20±0.99	13.27±0.96	14.03±0.97	13.99±0.83
Daily maximum	Tx_d	25.04±0.23	25.32±0.34	26.12±0.31	25.92±0.50
	Φ_{x_d}	13.97±0.09	13.35±0.09	13.52±0.06	13.23±0.07
Daily minimum	Tn_d	22.12±0.32	21.53±0.25	19.99±0.30	19.73±0.49
	Φ_{n_d}	5.55±0.06	4.894±0.06	4.72±0.08	4.28±0.08
DTR		2.92±0.35	3.79±0.27	6.12±0.43	6.19±0.58

Table 3 Linear trend in measurements taken at four Hong Kong meteorological stations.

Parameters		HKO (1885-2014)	KP (1993-2014)	TKL (1989-2014)	TYW (2000-2014)
Mean (°C per year)		**0.0118***	0.0070	0.0045	-0.0393
Annual Phase	(days per year)	**-0.0244***	-0.0175	0.0209	0.1369
	(rad. per year)	**-0.0004***	-0.0003	0.0003	0.0024
Annual Amplitude (°C per year)		-0.0018	0.0335	0.0122	0.0329
Semi-annual Phase	(days per year)	-0.0672	-0.6462	-0.1044	-0.2298
	(rad. per year)	-0.0023	-0.0222	-0.0036	-0.0079
Semi-annual Amplitude (°C per year)		0.0006	0.0054	**0.0287***	0.0109
Daily Phase	(hours per year)	**0.0136***	**0.0132***	**-0.0060***	-0.0070
	(rad. per year)	**0.0036***	**0.0035***	**-0.0016***	-0.0018
Daily Amplitude (°C per year)		0.0003	-0.0035	0.0044	-0.031
Semi-daily Phase	(hours per year)	**0.0093***	**0.0092***	-0.0029	-0.0049
	(rad. per year)	**0.0049***	**0.0048***	-0.0015	-0.0026
Semi-daily Amplitude (°C per year)		**0.0005***	-0.0031	0.0004	-0.0086

* Significant at the 0.01 level

Table 4 Pearson correlation coefficients of annual phase between four stations.

	HKO	KP	TKL	TYW
HKO	1	0.95*	0.85*	0.82*
KP	0.95*	1	0.84*	0.72*
TKL	0.85*	0.84*	1	0.92*
TYW	0.82*	0.72*	0.92*	1

*all significant at 0.01 level

Table 5 Pearson correlation coefficients of the daily phase between the four stations.

	HKO	KP	TKL	TYW
HKO	1	-0.24	-0.01	0.41
KP	-0.24	1	-0.22	0.26
TKL	-0.01	-0.22	1	0.62*
TYW	0.41	0.26	0.62*	1

*significant at 0.05 level

Table 6 Linear trends (°C per year) of the daily maximum temperature (*Tx_d*), daily minimum temperature (*Tn_d*) and DTR for different periods in HKO.

	Tx_d	*Tn_d*	DTR
1885-1959	**0.0140***	**0.0052***	**0.0087***
1960-1999	-0.0089	**0.0187***	**-0.0272***
2000-2014	0.0110	-0.0423	**0.0533***
1885-2014	**0.0123***	**0.0105***	0.0018

* Significant at the 0.01 level